ACS APPLIED MATERIALS & INTERFACES

Research Article

www.acsami.org

A Unique Type of Pyrrole-Based Cyanine Fluorophores with Turn-on and Ratiometric Fluorescence Signals at Different pH Regions for Sensing pH in Enzymes and Living Cells

Longwei He,[†] Weiying Lin,*[,†,‡] Qiuyan Xu,[†] and Haipeng Wei[†]

[†]State Key Laboratory of Chemo/Biosensing and Chemometrics, College of Chemistry and Chemical Engineering, Hunan University, Changsha, Hunan 410082, P. R. China

[‡]Institute of Fluorescent Probes for Biological Imaging, School of Chemistry and Chemical Engineering, School of Biological Science and Technology, University of Jinan, Jinan, Shandong 250022, P. R. China

Supporting Information

ABSTRACT: The development of new functional fluorescent dyes has attracted great attention. Herein we have described a novel strategy to design a unique type of cyanine dyes by attaching two indolium moieties at the α-positions of the pyrrole core. The new type of cyanine dyes is named as PyCy fluorophores. Importantly, PyCy dyes can exhibit an exceptional feature, fluorescence turn-on response at pH varying from acidic to near-neutral conditions, and a ratiometric fluorescence response at pH varying from near-neutral to basic conditions. By taking advantage of the fluorescence turn-on response of **PyCy2** at pH varying from acidic to near-neutral conditions and emission properties of **PyCy2**, we have demonstrated that a small-molecule fluorescent probe can image pH variations in living cells. Furthermore, we have demonstrated that **PyCy2** can sense real-time pH changes under alkaline conditions induced by enzymes based on the ratiometric fluorescence response of **PyCy2** at pH varying from near-neutral to basic conditions. We expect that the new design strategy for PyCy fluorophores may prompt the development of a wide variety of cyanine derivatives with desirable properties.

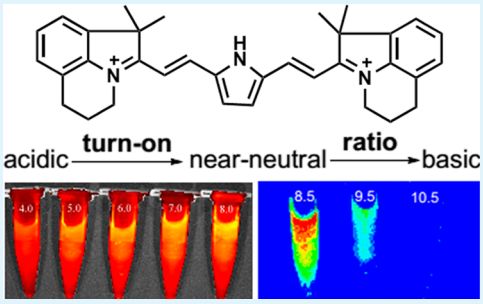

KEYWORDS: *cyanine dyes, pyrrole, pH probe, turn-on, ratiometric, fluorescence imaging*

1. INTRODUCTION

Pyrrole is often used as a building block for diverse array of dyes such as BODIPY, porphyrin, and carbazole (Scheme 1a).[1−3] Although pyrrole can be protonated and deprotonated with pK_{aH} and pK_a at −4.0 and 16.5,[4] respectively (Scheme 1b), these pK_{aH} and pK_a values may render pyrrole-based dyes unsuitable for sensing pH in many settings. However, it has been reported that the pK_a values of 2-nitropyrrole and 2,5-dinitropyrrole are 13.66 and 10.32,[5] respectively, indicating that electron-withdrawing groups at the α-positions of pyrrole could significantly decrease the pK_a. On the other hand, the indolium moiety is a typical electron-withdrawing group involved in many hemicyanine or cyanine fluorophores.[6−9]

Thus, we envisioned that attaching two indolium moieties at the α-positions of the pyrrole core may afford a new type of cyanine dyes, pyrrole-based cyanine (PyCy) fluorophores, and a representative example, **PyCy1**, is illustrated in Scheme 1c. We reasoned that this unique type of PyCy dyes may have a much higher pK_{aH} and lower pK_a when compared to the unmodified pyrrole due to the electron-withdrawing effects of two indolium moieties with positive charges. Obviously, like classic pyrroles, these novel PyCy dyes may exist in three different forms, protonated PyCy, PyCy, and deprotonated PyCy under different pH conditions. Importantly, we envisioned that the emission properties of three different forms of PyCy dyes may exhibit distinctive emission features. As shown in Scheme 1c, under near-neutral conditions, **PyCy1** may display strong fluorescence in light of its acceptor−donor−acceptor (A-D-A) conjugated system.[10,11] However, under protonation conditions, the nitrogen atom of the pyrrole core is protonated, and the A-D-A conjugated system is destroyed. We thus anticipated that the protonated **PyCy1** may show much weaker fluorescence when compared to **PyCy1**. Under deprotonation conditions, the deprotonated **PyCy1** has enhanced intramolecular charge transfer (ICT) character relative to **PyCy1**. Thus, the deprotonated **PyCy1** may exhibit a redshift in emission with respect to **PyCy1**. In other words, the fluorescence intensities and wavelengths of PyCy could be tuned under different pH conditions. From acidic to near-neutral conditions, we may observe a fluorescence turn-on signal, while from near-neutral to basic conditions, a ratiometric fluorescence signal may be detected. PyCy may exhibit this unique and advantageous feature. In sharp contrast, most small-molecule-based pH fluorescent probes show either a turn-on or ratiometric fluorescence signal over all the pH regions.

Intracellular pH regulates many cellular behaviors including ion transport,[12] endocytosis,[13] apoptosis,[14] and enzyme activity.[15]

Received: September 15, 2014
Accepted: November 19, 2014
Published: November 19, 2014

Scheme 1. Rational Design of a New Type of Pyrrole-Based Cyanine (PyCy) Dyes[a]

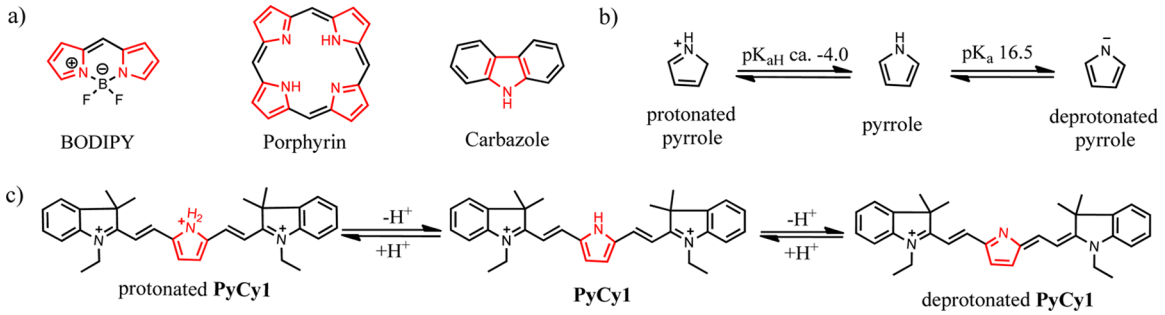

[a](a) Structures of some typical pyrrole-based dyes. (b) Pyrrole exists in three different forms. (c) **PyCy1**, a representative example of the novel class of PyCy dyes, may exist in three different forms, protonated **PyCy1**, **PyCy1**, and deprotonated **PyCy1** under different pH conditions. Notably, these three different forms may have distinct emission profiles.

Intracellular pH values of mammalian cells range from acidic in lysosomes to slightly basic in mitochondria. However, abnormal variations of pH in subcellular organelles, for instance, in mitochondria, may induce mitochondrial disorders[16] and cardiac dysfunction.[17] Unlike mammalian cells, extremophilic microbes are capable of survival in highly alkaline environments (pH roughly 7.0−12.0). They are classified in two broad categories: alkaline-tolerant organisms, which optimally grow in the pH range of 7.0−9.0, and alkalophilic organisms, which are ideally cultivated in the pH range of 10.0−12.0.[18] Alkaline enzymes produced by alkalophiles are also active in high pH environments. Alkaline cellulase, produced by alkalophilic bacillus sp. KSM-635, is most active at pH 9.5.[19] Fluorescent probes have attracted great attention, as they can be used as powerful tools for detection of biologically relevant analytes.[20−22] A large number of fluorescent probes suitable for sensing pH under typical physiological conditions have been developed.[23−26] However, few of them are capable of sensing pH under alkaline conditions, especially monitoring pH changes induced by alkaline enzymes. Thus, to expand the utility of the fluorescent probes, pH probes need to be developed that cover not only the typical physiological regions but also the basic regions.

2. EXPERIMENTAL SECTION

2.1. Materials and Instruments. Pyrrole-2,5-dicarbaldehyde[27] (**1**) and 5,6,6-trimethyl-1,2,3,6-tetrahydropyrolo[3,2,1-*ij*]-quinolinium[28] (**3**) were synthesized according to previous work. Unless otherwise stated, all reagents were purchased from commercial suppliers and used without further purification. Solvents used were purified by standard methods prior to use. Twice-distilled water was used throughout all experiments. High resolution mass spectrometric (HRMS) analyses were performed on a Finnigan MAT 95 XP spectrometer, NMR spectra were recorded on an INOVA-400 spectrometer, using TMS as an internal standard, electronic absorption spectra were obtained on a LabTech UV Power spectrometer, photoluminescent spectra were recorded with a Hitachi F4600 fluorescence spectrophotometer with a 1 cm standard quartz cell, the fluorescence imaging of cells was performed with an Olympus FV1000 (TY1318) confocal microscope, the fluorescence imaging of solutions was performed with an IVIS Lumina XR (IS1241N6071) in vivo imaging system, the pH measurements were carried out on a Mettler-Toledo Delta 320 pH meter, TLC analysis was performed on silica gel plates, and column chromatography was conducted over silica gel (mesh 200−300) (silica gel and silica gel plates were obtained from Qingdao Ocean Chemicals).

2.2. Preparation of the Stock and Test Solution. The stock solution of compounds **PyCy1−3** was prepared at 500 μM in MeOH. The test solution of compounds **PyCy1−3** was prepared by mixing 60 μL of stock solution (500 μM), 2.85 mL of PBS, and 90 μL of MeOH. The stock solution of *p*-nitrophenyl phosphate (PNPP) was prepared at 100 mM in twice-distilled water. The test solution of PNPP was prepared by mixing 150 μL of stock solution (100 mM) and 2.70 mL of Tris buffer. The stock solutions of metal ions for selectivity experiments were prepared, respectively, by dissolving NaCl, KCl, $CaCl_2$, $ZnCl_2$, $AlCl_3{\cdot}6H_2O$, $HgCl_2$, $AgNO_3$, $MgCl_2{\cdot}6H_2O$, $FeCl_2{\cdot}4H_2O$, $FeCl_3{\cdot}6H_2O$, $MnCl_2{\cdot}4H_2O$, $CuCl_2{\cdot}2H_2O$, $PbCl_2$, $NiCl_2{\cdot}6H_2O$, and $CdCl_2{\cdot}{}^1/_2H_2O$ in twice-distilled water. The slight pH variations of the solutions were achieved by adding minimum volumes of NaOH (0.1 M) or HCl (0.2 M).

2.3. Determination of the Fluorescence Quantum Yield. Fluorescence quantum yields for **PyCy1−3** were determined by using rhodamine B (Φ_f = 0.31 in water) in acetone or ICG (Φ_f = 0.13 in DMSO) in ethanol as a fluorescence standard.[29,30] The quantum yield was calculated using the following eq 1:

$$\Phi_{F(X)} = \Phi_{F(S)}(A_S F_X / A_X F_S)(n_X / n_S)^2 \quad (1)$$

where Φ_F is the fluorescence quantum yield, A is the absorbance at the excitation wavelength, F is the area under the corrected emission curve, and n is the refractive index of the solvents used. Subscripts S and X refer to the standard and to the unknown, respectively.

2.4. Calculation of pK_a and pK_{aH} Values. pK_a values of PyCy dyes at acidic to near-neutral pH regions were calculated by regression analysis of the fluorescence data to fit eq 2, and pK_{aH} values of PyCy dyes at the basic pH region were calculated by eq 3:[31]

$$\mathrm{pH} - \mathrm{p}K_a = \log(F_{max} - F)/(F - F_{min}) \quad (2)$$

where F is the area under the corrected emission curve, and F_{max} and F_{min} are maximum and minimum limiting values of F, respectively.

$$\mathrm{pH} - \mathrm{p}K_{aH} = c[\log(R - R_{min})/(R_{max} - R)] + \log(I_a/I_b) \quad (3)$$

where R is the ratio of emission intensity at two wavelengths, R_{max} and R_{min} are maximum and minimum limiting values of R, c is the slope (positive for the basic forms of the dyes and negative for the acidic forms), and I_a/I_b is the ratio of the absorption intensity in acid to the absorption intensity in base at the wavelength chosen for the denominator of R.

2.5. EC 109 Cell Culture and Imaging of pH Variations Using Probe PyCy2. EC109 cells were cultured in DMEM (Dulbecco's modified Eagle medium) supplemented with 10% FBS (fetal bovine serum) in an atmosphere of 5% CO_2 and 95% air at 37 °C. For detection of pH, EC109 cells were incubated with 5.0 μM **PyCy2** for 20 min in an atmosphere of 5% CO_2 and 95% air and then washed with PBS medium of varying pH values (pH 4.0−8.0) containing nigericin (1 μg/mL) three times, followed by incubating with the corresponding PBS for another 15 min. Subsequently, the cells were imaged using an Olympus FV1000 (TY1318) confocal microscope with an excitation filter of 559 nm and emission collection between 610 and 665 nm.

2.6. Detection of pH Changes Induced by *Escherichia coli* Alkaline Phosphatase in Alkaline Aqueous Solution. The enzymatic reaction was carried out in 10 mM Tris buffer (pH 10.0, 0.5 M NaCl).

Two units of *Escherichia coli* alkaline phosphatase was added to the Tris buffer containing 10 μM **PyCy2** and 5 mM *p*-nitrophenyl phosphate to start the hydrolysis reaction. The changes of fluorescence were recorded within 10 min using a Hitachi F4600 fluorescence spectrophotometer with excitation at 598 nm.

2.7. Cytotoxicity Assays. HeLa cells were grown in modified Eagle's medium (MEM) supplemented with 10% FBS (fetal bovine serum) in an atmosphere of 5% CO_2 and 95% air at 37 °C. Immediately before the experiments, the cells were placed in a 96-well plate, followed by addition of increasing concentrations of dyes **PyCy1−3** (99% MEM and 1% DMSO). The final concentrations of **PyCy1−3** were 5, 10, 20 μM (n = 5), respectively. The cells were then incubated at 37 °C in an atmosphere of 5% CO_2 and 95% air at 37 °C for 24 h, followed by MTT assays. An untreated assay with MEM (n = 5) was also conducted under the same conditions.

2.8. Synthesis of Compounds PyCy1−3. A mixture of pyrrole-2,5-dicarbaldehyde (20 mg, 0.16 mmol), indolium iodate **2**, **3**, or **4** (0.64 mmol), and sodium acetate (39 mg, 0.48 mmol) in acetic anhydride (3 mL) was refluxed at 80 °C for 2.0 h. Then water (3 mL) was added to the reaction mixture to quench the reaction. The solvent was removed under reduced pressure to give the crude products, which were purified by silica gel flash chromatography using CH_2Cl_2 to CH_2Cl_2/ethanol (50:1 to 5:1) as eluent to afford the corresponding PyCy compounds (99.1 mg, 86.4% yield for **PyCy1**, 97.6 mg, 82.3% yield for **PyCy2**, and 114.8 mg, 87.8% yield for **PyCy3**) as dark purple solids. **PyCy1**: ^{1}H NMR (400 MHz, $CDCl_3$): 1.63 (t, J = 6.8 Hz, 6H), 1.91 (s, 12H), 4.91−4.93 (4H), 7.54−7.58 (m, 7H), 7.71 (s, 2H), 8.16−8.20 (d, J = 15.6 Hz, 2H), 8.30−8.37 (m, 1H), 8.41−8.47 (2H), 13.24 (s, 1H); ^{13}C NMR (100 MHz, $CDCl_3$): 14.52, 27.02, 43.36, 52.17, 113.86, 123.00, 129.47, 129.52, 140.34, 141.14, 143.95, 180.53, MS (ESI) m/z 462.2 [M$^+$]. HRMS (ESI) m/z calcd for $C_{32}H_{36}N_3$ (M$^+$): 462.2904. Found 462.2887. **PyCy2**: ^{1}H NMR (400 MHz, $CDCl_3$): 1.91 (s, 12H), 2.42 (4H), 3.01 (4H), 4.93 (4H), 7.29 (s, 2H), 7.34−7.36 (d, J = 7.2 Hz, 2H), 7.39−7.43 (t, J = 7.2 Hz, 2H), 7.62 (s, 2H), 8.05−8.09 (d, J = 16.0 Hz, 2H), 8.35−8.39 (d, J = 16.0 Hz, 2H), 12.85 (s, 1H); ^{13}C NMR (100 MHz, $CDCl_3$): 21.72, 23.56, 26.67, 48.95, 53.03, 53.52, 111.91, 120.42, 127.57, 127.96, 129.29, 137.60, 138.72, 139.38, 142.58, 178.68. MS (EI) m/z 486.2[M$^+$]. HRMS (EI) m/z calcd for $C_{34}H_{36}N_3$ (M$^+$): 486.2904, Found 486.2887. **PyCy3**: ^{1}H NMR (400 MHz, $CDCl_3$): 1.69−1.72 (t, J = 6.8 Hz, 6H), 2.21 (s, 12H), 5.09−5.11 (4H), 7.65−7.69 (t, J = 8.4 Hz, 4H), 7.75−7.78 (t, J = 6.8 Hz, 2H), 7.90 (s, 2H), 8.05 (d, J = 8.0 Hz, 2H), 8.10 (d, J = 8.8 Hz, 2H), 8.19−8.23 (d, J = 16.0 Hz, 2H), 8.29 (d, J = 8.4 Hz, 2H), 8.65−8.68 (d, J = 14.8 Hz, 2H), 13.12 (s, 1H). ^{13}C NMR (100 MHz, $CDCl_3$): 14.92, 27.01, 43.80, 53.79, 99.99, 108.26, 111.51, 123.05, 127.57, 128.72, 130.23, 131.72, 133.54, 137.62, 139.19, 140.02, 181.25. MS (EI) m/z 562.3 [M$^+$]. HRMS (EI) m/z calcd for $C_{40}H_{40}N_3$ (M$^+$): 562.3217. Found 562.3204.

Scheme 2. Synthesis of Pyrrole-Based Cyanine Dyes PyCy1−3

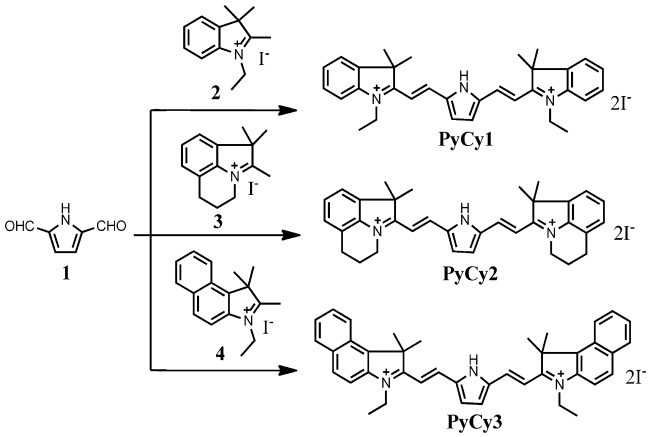

3. RESULTS AND DISCUSSION

3.1. Design and Synthesis of Compounds PyCy1−3. To demonstrate the feasibility of the aforementioned strategy for development of **PyCy** dyes as unique candidates for fluorescent pH probes, we decided to construct **PyCy1−3** dyes, which contain indolium, tetrahydropyrroloquinolinium, or benzindolium moieties, respectively (Scheme 2). Pyrrole-2,5-dicarbaldehyde (**1**) reacted with 1-ethyl-2,3,3-trimethyl-3*H*-indolium (**2**), 5,6,6-trimethyl-1,2,3,6-tetrahydropyrrolo[3,2,1-*ij*]-quinolinium (**3**), or 3-ethyl-1,1,2-trimethyl-1*H*-benzo[*e*]-indolium (**4**) in acetic anhydride, affording **PyCy1**, **PyCy2**, or **PyCy3**, respectively. The structures of **PyCy1−3** were characterized by ^{1}H NMR, ^{13}C NMR, MS, and HRMS (see the Supporting Information).

3.2. Optical Properties of PyCy1−3. With the desired compounds in hand, we first proceeded to examine their absorption and emission properties in organic solvents such as MeOH, EtOH, CH_2Cl_2, CH_3CN, CH_3COCH_3, DMF, and DMSO. The absorption and emission profiles are shown in Figure 1 and Figures S1 and S2, Supporting Information, and the corresponding photophysical data are compiled in Tables S1 and S2. Both the absorption and emission wavelengths are solvent-dependent. We then preliminarily investigated their optical properties in PBS buffer solutions at three different pH values. In the case of **PyCy1**, at pH 7.4, the dye displayed intense emission at 638 nm (Figure 2b). However, at pH 4.5, a marked drop in the emission in the same wavelength was observed. In sharp contrast, at pH 10.5, a new intense emission

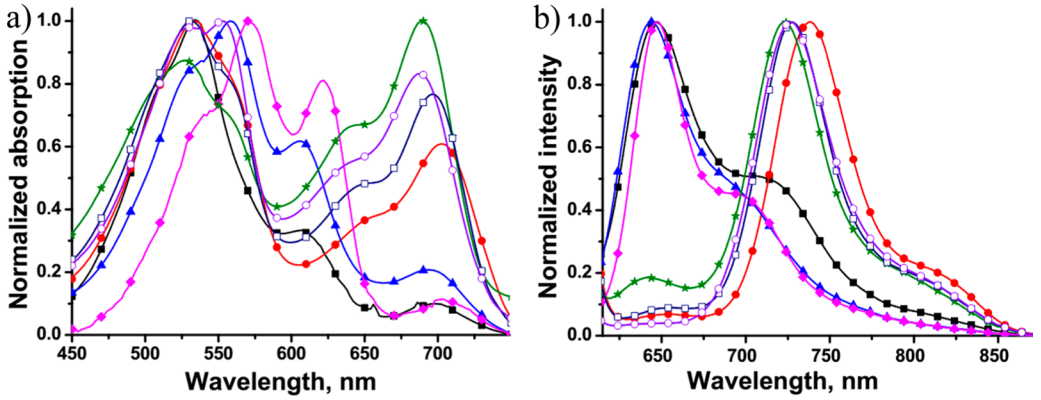

Figure 1. Absorption (a) and fluorescence (b) spectra of compound **PyCy1** (10 μM) in distinct organic solvents such as DMF (■), DMSO (●), acetone (▲), DCM (◆), MeOH (★), EtOH (□), and MeCN (○).

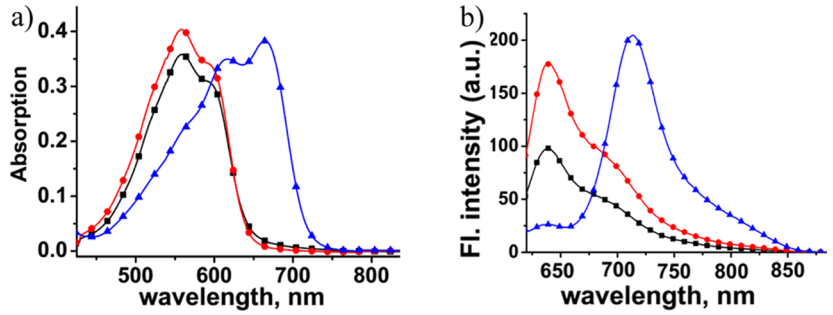

Figure 2. Absorption (a) and fluorescence (b) spectra of compound **PyCy1** (10 μM) in various PBS solutions (5% MeOH, pH 4.5 (■), 7.4 (●), and 10.5 (▲), respectively). The excitation wavelength is at 594 nm.

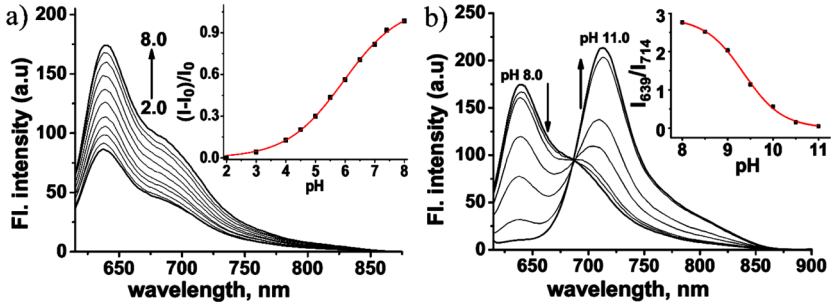

Figure 3. Fluorescence spectra of 10 μM **PyCy2** in 25 mM PBS (containing 5% MeOH) with pH varying (a) from 2.0 to 8.0 and (b) from 8.0 to 11.0 upon excitation at 598 nm. Insets: (a) Plot of $(I - I_0)/I_0$ versus pH. I_0 and I denote the intensities of the emission peak at pH 2.0 and at any pH from 2.0 to 8.0. (b) Plot of I_{639}/I_{714} versus pH. I_{639} and I_{714} denote the emission intensities at 639 and 714 nm, respectively.

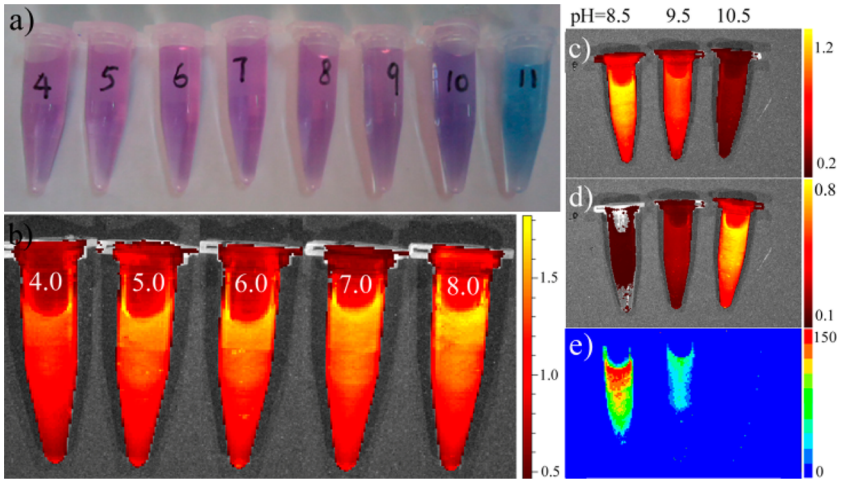

Figure 4. Visual pictures and fluorescent images of 10 μM **PyCy2** (PBS containing 5% MeOH) at different pH values. (a) The visual colors of **PyCy2** at pH 4.0 to 11.0 under natural light. (b) The fluorescent images of **PyCy2** at pH 4.0 to 8.0 upon excitation at 535 nm. The fluorescent images of **PyCy2** at pH 8.5 to 10.5 were collected via (c) a DsRed filter (excited at 535 nm) and (d) a Cy5.5 filter (excited at 640 nm), respectively. (e) Pseudocolored ratiometric images ($I_{DsRed}/I_{Cy5.5}$) of **PyCy2** at pH from 8.5 to 10.5. The number indicates the pH value of the corresponding solution.

peak at 714 nm appeared. Similar phenomena were also observed for the **PyCy2** and -**3** dyes (Figure S3 and S4, Supporting Information), indicating that PyCy dyes may exhibit different patterns of fluorescence signals (variations in fluorescence intensity or wavelength) at different pH regions.

Encouraged by the above promising preliminary results, we then decided to examine the patterns of fluorescence signals of PyCy dyes by titrating the dyes in more detail. As shown in Figure 3a, the emission intensity of **PyCy2** increased gradually from pH 2.0 to 8.0 at 639 nm in 25 mM PBS. Thus, a fluorescence turn-on signal was observed. However, when **PyCy2** was titrated with pH varying from 8.0 to 11.0, the fluorescence intensity of the peak at 639 nm decreased and simultaneously a new strong peak at 714 nm appeared (Figure 3b). Notably, a distinct isoemissive point at 685 nm was observed, reinforcing the observation that **PyCy2** displayed a ratiometric signal under basic conditions. The changes in the absorption profiles (Figure S5b, Supporting Information) are in good agreement with the variations in the emission profiles.

The visual color and fluorescence images of the **PyCy2** solution under different pH values are displayed in Figure 4. The **PyCy2** solution exhibited a pink color under acidic and

near-neutral conditions; however, it turned blue under alkaline conditions (Figure 4a). As illustrated in Figure 4b, the fluorescence became brighter with pH increasing from 4.0 to 8.0 (as indicated by the scale bar beside the images). In contrast, a ratiometric pattern for the images was noted under basic conditions (pH 8.5−10.5) (Figure 4c−e). The changes in the fluorescence images are in accordance with the above spectral results, suggesting that, as designed, **PyCy2** could show turn-on and ratiometric signals at different regions of pH.

The selectivity of sensor **PyCy2** to H^+ over metal ions was investigated. When some physiologically important metal ions, such as K^+, Na^+, Ca^{2+}, Mg^{2+}, Cu^{2+}, and Fe^{3+}, were added to the solution of sensor **PyCy2**, only negligible changes of emission intensity were observed (Figure 5). In addition, common nucleophilic agents such as Cys and GSH also have little effect on **PyCy2**. In contrast, H^+ induced a clear increase in emission intensity at 638 nm, indicating that the sensor **PyCy2** has a moderate selectivity for H^+ over other analytes. We then examined the reversibility of **PyCy2** for sensing pH. Alternative addition of NaOH and HCl was employed to adjust the pH values of the aqueous solution. The emission at 639 nm decreased from pH 8.0 to 4.5, but the emission recovered with pH increasing from 4.5 to 8.0 (Figure S6a, Supporting Information). Under basic conditions, the ratio (I_{639}/I_{714}) decreased from pH 8.0 to 10.5, but the ratio recovered when pH dropped from 10.5 to 8.0 (Figure S6b, Supporting Information). The processes can be repeated for at least five cycles.

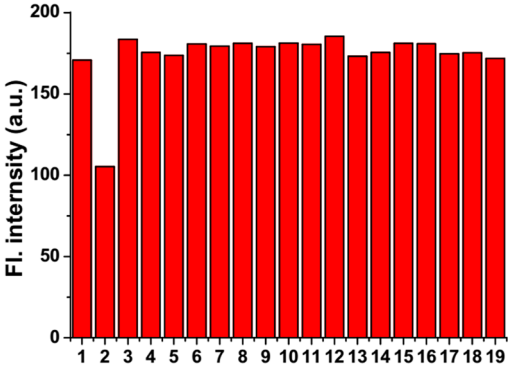

Figure 5. Fluorescence intensity (at 638 nm) of sensor **PyCy2** (10 μM) in the presence of various analytes in PBS buffer (pH 7.4, containing 5% MeOH as a cosolvent). 1, blank; 2, H^+ (pH = 4.5); 3, K^+ (50 mM); 4, Na^+ (50 mM); 5, Ag^+ (200 μM); 6, Ca^{2+} (2 mM); 7, Cd^{2+} (200 μM); 8, Fe^{2+} (200 μM); 9, Ni^{2+} (200 μM); 10, Cu^{2+} (200 μM); 11, Mg^{2+} (2 mM); 12, Mn^{2+} (200 μM); 13, Zn^{2+} (200 μM); 14, Pb^{2+} (200 μM); 15, Hg^{2+} (200 μM); 16, Fe^{3+} (2 mM); 17, Al^{3+} (200 μM); 18, Cys (200 μM); 19, GSH (200 μM).

Like **PyCy2**, **PyCy1** and **PyCy3** also exhibited a turn-on pattern from acidic to near-neutral conditions and a ratiometric pattern from near-neutral to basic conditions (Figure S7, Supporting Information). However, the changes in ratios for **PyCy3** are inferior to those for **PyCy1** and **PyCy2**. On the basis of the data in Figure S7, the pK_{aH} and pK_a values for **PyCy1**, **PyCy2**, and **PyCy3** were determined as 5.18/9.35, 5.74/9.39, and 3.89/9.66, respectively. Both the pK_{aH} and pK_a values for **PyCy2** are slightly higher than those for **PyCy1**. For these two reasons, we decided to select **PyCy2** as a pH probe candidate to further evaluate its potential use in living cells and alkaline enzymes.

3.3. Fluorescence pH Imaging in Living Cells. The standard MTT assays indicate that **PyCy2** has negligible cytotoxicity to living cells (Figure S8, Supporting Information), suggesting that **PyCy2** may be suitable for cell imaging. EC 109 cells were colabeled with **PyCy2** and Mito Tracker Green, a commercial labeling dye specific for mitochondria. As shown in Figure 6, the red and green fluorescent images overlapped well with a Pearson's colocalization coefficient = 0.90, indicating that **PyCy2** primarily located in the mitochondria

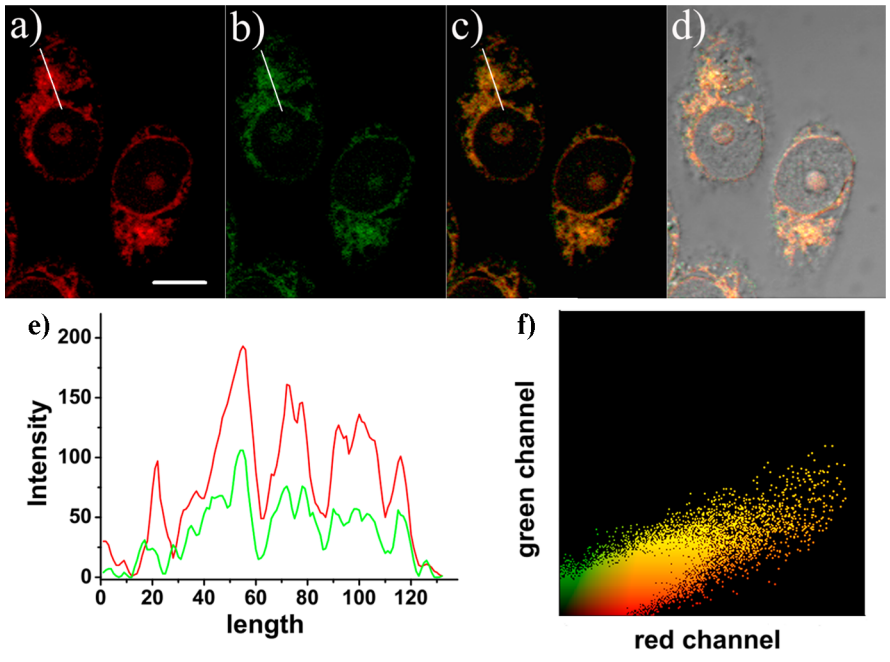

Figure 6. Confocal fluorescence images of EC 109 cells stained with (a) **PyCy2** (5 μM) collected between 610 and 665 nm upon excitation at 559 nm and (b) Mito Tracker Green (2 μM) collected between 509 and 556 nm upon excitation at 488 nm. (c) Merged image of a and b. (d) Merged image of c and bright-field image. (e) Intensity profile of the region of interest (indicated by the white color line in a and b) across the EC 109 cells. Red line for a and green line for b. (f) Correlation plot of **PyCy2** and Mito Tracker Green intensities. Scale bar = 10 μm.

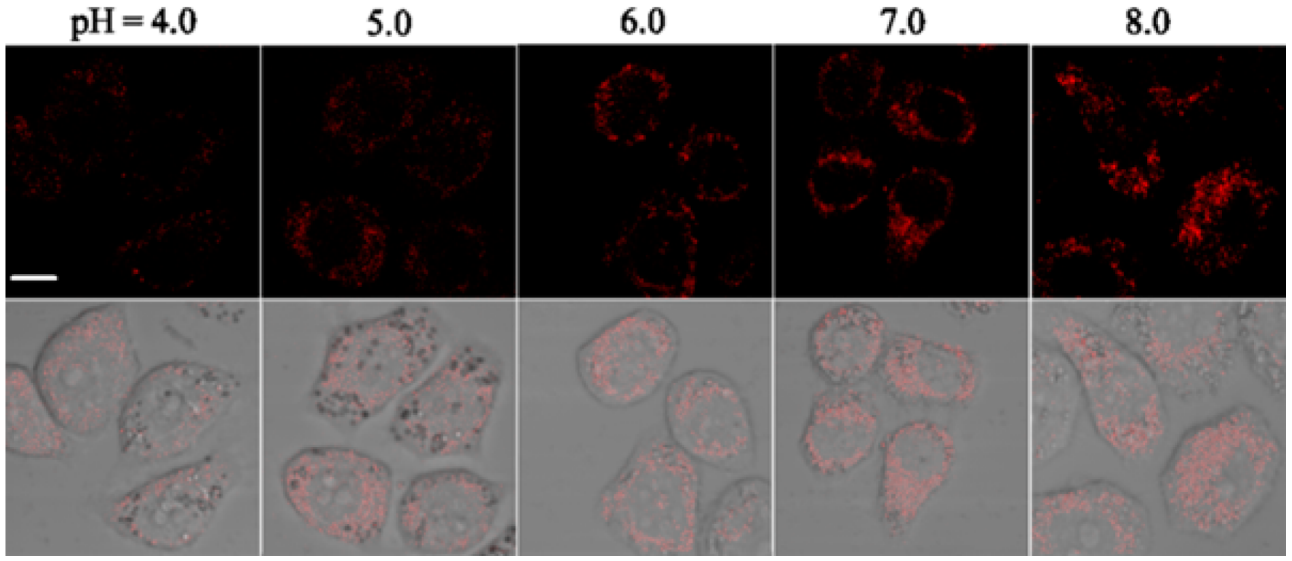

Figure 7. Confocal fluorescence images of EC 109 cells stained with **PyCy2** (5 μM) in a PBS medium of varying pH (pH 4.0−8.0) with the addition of nigericin (1 μg/mL). The top row images of fluorescence emission were collected between 610 to 665 nm upon excitation at 559 nm. The bottom row images are the result of merging the top images and the corresponding bright-field images. Scale bar = 10 μm.

likely due to its positively charged structure.[32] We thus then monitored the pH changes in the mitochondria. Nigericin is often used to promote equilibration of external and internal mitochondrion pH.[33,34] After incubation with **PyCy2** (5.0 μM) for 20 min, the EC 109 cells were washed in PBS medium of varying pH (pH 4.0−8.0) containing nigericin (1 μg/mL). The dye-stained cells displayed the weakest fluorescence at pH 4.0 and the brightest fluorescence at pH 8.0 (Figure 7), which is in good agreement with the fluorescence spectra of **PyCy2** in aqueous solution at a similar pH region (Figure 3a).

3.4. Real-Time Sensing of pH Changes in Enzymes under Alkaline Conditions. We further proceeded to examine the possibility of **PyCy2** for sensing real-time pH changes under alkaline conditions induced by enzymes. *Escherichia coli* alkaline phosphatase (EC 3.1.3.1), most effective in an alkaline environment, can catalyze hydrolysis of aryl phosphate substrates, for instance, *p*-nitrophenyl phosphate (PNPP), to produce inorganic phosphate and *p*-nitrophenol.[35,36] This enzymatic hydrolysis may induce a slight pH decrease. Thus, we wondered whether **PyCy2** could detect the real-time minor pH changes elicited by the hydrolysis of PNPP. Toward this end, a stock solution of PNPP (5 mM) was added into a Tris buffer (25 mM, pH 10.0, 0.5 M NaCl) containing **PyCy2** (10 μM), followed by addition of 2 U of alkaline phosphatase to start the enzymatic hydrolysis. As shown in Figure 8, the ratiometric changes in the emission spectra were time-dependent. With the enhancement of the incubation time, a drop of the emission peak at 714 nm and a simultaneous increase of the emission peak at 639 nm were observed. Notably, a clear isoemissive point appeared at 683 nm (Figure 8), which is in good agreement with that observed for titrating **PyCy2** under basic conditions (Figure 3b), indicating that, even in the presence of the *Escherichia coli* alkaline phosphatase, the probe continued to function in a similar ratiometric fashion. The real-time changes of the emission intensity ratios at 639 and 714 nm (inset of Figure 8) are consistent with the fact that the hydrolysis of PNPP to inorganic phosphate and phenol can induce a decrease of pH. The final pH value of the reaction mixture was calculated as 9.70 via the linear relationship obtained in the

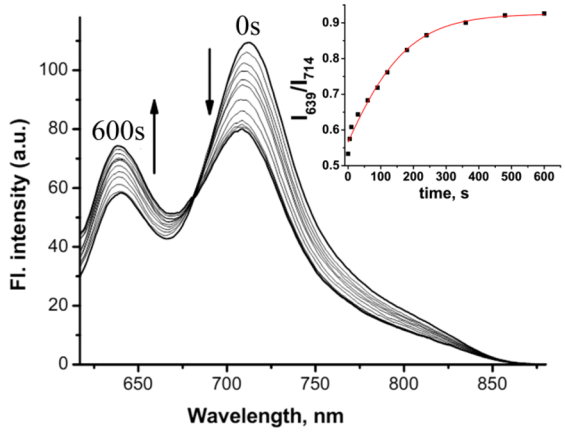

Figure 8. Incubation time-dependent changes of the fluorescence spectra of 10 μM **PyCy2** in Tris solution (25 mM, pH 10.0) containing 5 mM PNPP and 2 U of *Escherichia coli* alkaline phosphatase. The excitation wavelength is at 598 nm. Inset: Plot of I_{639}/I_{714} versus the incubation time. I_{639} and I_{714} denote the emission intensities at 639 and 714 nm, respectively.

alkaline buffers, which is almost identical to 9.65 ± 0.04 measured by a pH meter. Thus, the probe **PyCy2** can detect very minor pH variations under alkaline conditions in real-time, suggesting that the probe could be a potential molecular tool not only for assaying alkaline enzyme activities but also for detecting pH changes in alkaline microorganisms.

4. CONCLUSION

In summary, we have introduced a new strategy to construct a unique class of pyrrole-based cyanine dyes, PyCy fluorophores, by attaching two indolium moieties at the α-positions of the pyrrole core. Importantly, PyCy dyes could exhibit a fluorescence turn-on response at pH varying from acidic to near-neutral conditions, and a ratiometric fluorescence response at pH varying from near-neutral to basic conditions. Interestingly, this is the first class of fluorescent pH probes with this fascinating property. We further demonstrated that this remarkable feature of these novel dyes rendered them suitable

for monitoring pH variations in living cells and animals with a turn-on mode and real-time sensing of pH changes induced by alkaline phosphatase with a ratiometric mode. We expect that the design strategy of PyCy fluorophores may prompt the development of a wide variety of cyanine derivatives with unique properties.

■ ASSOCIATED CONTENT

Ⓢ Supporting Information

Experimental procedures, some spectra, photophysical data, MTT assay, and characterization spectra. This material is available free of charge via the Internet at http://pubs.acs.org.

■ AUTHOR INFORMATION

Corresponding Author

*E-mail: weiyinglin2013@163.com.

Notes

The authors declare no competing financial interest.

■ ACKNOWLEDGMENTS

Funding was partially provided by NSFC (21172063, 21472067) and a startup fund from University of Jinan.

■ REFERENCES

(1) Boens, N.; Leen, V.; Dehaen, W. Fluorescent Indicators Based on BODIPY. *Chem. Soc. Rev.* **2012**, *41*, 1130−1172.

(2) Wood, T. E.; Thompson, A. Advances in the Chemistry of Dipyrrins and Their Complexes. *Chem. Rev.* **2007**, *107*, 1831−1861.

(3) Zhang, X.; Wang, C.; Jin, L.; Han, Z.; Xiao, Y. Photostable Bipolar Fluorescent Probe for Video Tracking Plasma Membranes Related Cellular Processes. *ACS Appl. Mater. Interfaces* **2014**, *6*, 12372−12379.

(4) Glayden, J.; Greeves, N.; Warren, S.; Wother, P. *Organic Chemistry*; Oxford University Press: Cary, NC, 2000; p 203 and p 1164.

(5) CAS registry numbers 5919-26-6 and 114536-31-1 from https://scifinder.cas.org/scifinder/view/scifinder/scifinderExplore.jsf.

(6) Chen, S.; Hong, Y.; Liu, Y.; Liu, J.; Leung, C. W. T.; Li, M.; Kwok, R. T. K.; Zhao, E.; Lam, J. W. Y.; Yu, Y.; Tang, B. Z. Full-Range Intracellular pH Sensing by an Aggregation-Induced Emission-Active Two-Channel Ratiometric Fluorogen. *J. Am. Chem. Soc.* **2013**, *135*, 4926−4929.

(7) Chen, Y.; Zhu, C.; Yang, Z.; Chen, J.; He, Y.; Jiao, Y.; He, W.; Qiu, L.; Cen, J.; Guo, Z. A Ratiometric Fluorescent Probe for Rapid Detection of Hydrogen Sulfide in Mitochondria. *Angew. Chem., Int. Ed.* **2013**, *52*, 1688−1691.

(8) Huang, X.; Gu, X.; Zhang, G.; Zhang, D. A Highly Selective Fluorescence Turn-on Detection of Cyanide Based on the Aggregation of Tetraphenylethylene Molecules Induced by Chemical Reaction. *Chem. Commun.* **2012**, *48*, 12195−12197.

(9) Zheng, H.; Yan, M.; Fan, X.-X.; Sun, D.; Yang, S.-Y.; Yang, L.-J.; Li, J.-D.; Jiang, Y.-B. A Heptamethine Cyanine-Based Colorimetric and Ratiometric Fluorescent Chemosensor for the Selective Detection of Ag^+ in an Aqueous Medium. *Chem. Commun.* **2012**, *48*, 2243−2245.

(10) Feng, X. J.; Wu, P. L.; Bolze, F.; Leung, H. W. C.; Li, K. F.; Mak, N. K.; Kwong, D. W. J.; Nicoud, J.-F.; Cheah, K. W.; Wong, M. S. Cyanines as New Fluorescent Probes for DNA Detection and Two-Photon Excited Bioimaging. *Org. Lett.* **2010**, *12*, 2194−2197.

(11) Yang, L.; Li, X.; Yang, J.; Qu, Y.; Hua, J. Colorimetric and Ratiometric Near-Infrared Fluorescent Cyanide Chemodosimeter Based on Phenazine Derivatives. *ACS Appl. Mater. Interfaces* **2013**, *5*, 1317−1326.

(12) Varadi, A.; Rutter, G. A. Ca^{2+}-Induced Ca^{2+} Release in Pancreatic Islet β-Cells: Critical Evaluation of the Use of Endoplasmic Reticulum-Targeted "Cameleons". *Endocrinology* **2004**, *145*, 4540−4549.

(13) Ohkuma, S.; Poole, B. Fluorescence Probe Measurement of the Intralysosomal pH in Living Cells and the Perturbation of pH by Various Agents. *Proc. Natl. Acad. Sci. U. S. A.* **1978**, *75*, 3327−3331.

(14) Ishaque, A.; Al-Rubeai, M. Use of Intracellular pH and Annexin-V Flow Cytometric Assays to Monitor Apoptosis and Its Suppression by Bcl-2over-expression in Hybridoma Cell Culture. *J. Immunol. Methods* **1998**, *221*, 43−57.

(15) Pérez-Sala, D.; Collado-Escobar, D.; Mollinedo, F. Intracellular Alkalinization Suppresses Lovastatin-Induced Apoptosis in HL-60 Cells Through the Inactivation of a pH-Dependent Endonuclease. *J. Biol. Chem.* **1995**, *270*, 6235−6242.

(16) Gardner, A.; Boles, R. G. Is a "Mitochondrial Psychiatry" in the Future? A Review. *Curr. Psychiatry Rev.* **2005**, *1*, 255−271.

(17) Lesnefsky, E. J.; Moghaddas, S.; Tandler, B.; Kerner, J.; Hoppel, C. L. Mitochondrial Dysfunction in Cardiac Disease: Ischemia−Reperfusion, Aging, and Heart Failure. *J. Mol. Cell Cardiol.* **2001**, *33*, 1065−1089.

(18) Krulwich, T. A.; Guffanti, A. A. Alkalophilic Bacteria. *Annu. Rev. Microbiol.* **1989**, *43*, 435−463.

(19) Ito, S. Alkaline Cellulases from Alkaliphilic Bacillus: Enzymatic Properties, Genetics, and Application to Detergents. *Extremophiles* **1997**, *1*, 61−66.

(20) Yang, Y.; Zhao, Q.; Feng, W.; Li, F. Luminescent Chemodosimeters for Bioimaging. *Chem. Rev.* **2013**, *113*, 192−270.

(21) Cheng, X.; Tang, R.; Jia, H.; Feng, J.; Qin, J.; Li, Z. New Fluorescent and Colorimetric Probe for Cyanide: Direct Reactivity, High Selectivity, and Bioimaging Application. *ACS Appl. Mater. Interfaces* **2012**, *4*, 4387−4392.

(22) Lu, X.; Guo, Z.; Feng, M.; Zhu, W. Sensing Performance Enhancement via Acetate-Mediated N-Acylation of Thiourea Derivatives: A Novel Fluorescent Turn-On Hg^{2+} Chemodosimeter. *ACS Appl. Mater. Interfaces* **2012**, *4*, 3657−3662.

(23) Han, J.; Burgess, K. B. Fluorescent Indicators for Intracellular pH. *Chem. Rev.* **2010**, *110*, 2709−2728.

(24) Peng, X.; Song, F.; Lu, E.; Wang, Y.; Zhou, W.; Fan, J.; Gao, Y. Heptamethine Cyanine Dyes with a Large Stokes Shift and Strong Fluorescence: A Paradigm for Excited-State Intramolecular Charge Transfer. *J. Am. Chem. Soc.* **2005**, *127*, 4170−4171.

(25) Tang, B.; Yu, F.; Li, P.; Tong, L.; Duan, X.; Xie, T.; Wang, X. A Near-Infrared Neutral pH Fluorescent Probe for Monitoring Minor pH Changes: Imaging in Living HepG2 and HL-7702 Cells. *J. Am. Chem. Soc.* **2009**, *131*, 3016−3023.

(26) Ke, G.; Zhu, Z.; Wang, W.; Zou, Y.; Guan, Z.; Jia, S.; Zhang, H.; Wu, X.; Yang, C. J. A Cell-Surface-Anchored Ratiometric Fluorescent Probe for Extracellular pH Sensing. *ACS Appl. Mater. Interfaces* **2014**, *6*, 15329−15334.

(27) Knizhnikov, V. A.; Borisova, N. E.; Yurashevich, N. Y.; Popova, L. A.; Chernyad'ev, A. Y.; Zubreichuk, Z. P.; Reshetova, M. D. Pincer Ligands Based on α-Amino Acids: I. Synthesis of Polydentate Ligands from Pyrrole-2,5-dicarbaldehyde. *Russ. J. Org. Chem.* **2007**, *43*, 855−860.

(28) Zimmermann, T.; Brede, O. 3H-Indolium Salts Efficiently Prepared from N-Substituted Anilines and α-Branched Ketones by a One-Pot Synthesis. *J. Heterocycl. Chem.* **2004**, *41*, 103−108.

(29) Magde, D.; Rojas, G. E.; Seybold, P. Solvent Dependence of the Fluorescence Lifetimes of Xanthene Dyes. *Photochem. Photobiol.* **1999**, *70*, 737−744.

(30) Oushiki, D.; Kojima, H.; Terai, T.; Arita, M.; Hanaoka, K.; Urano, Y.; Nagano, T. Development and Application of a Near-Infrared Fluorescence Probe for Oxidative Stress Based on Differential Reactivity of Linked Cyanine Dyes. *J. Am. Chem. Soc.* **2010**, *132*, 2795−2801.

(31) Whitaker, J. E.; Haugland, R. P.; Prendergast, F. G. Spectral and Photophysical Studies of Benzo[c]xanthene Dyes: Dual Emission pH Sensors. *Anal. Biochem.* **1991**, *194*, 330−344.

(32) Hoye, A. T.; Davoren, J. E.; Wipf, P. Targeting Mitochondria. *Acc. Chem. Res.* **2008**, *41*, 87−97.

(33) Soltoff, S. P.; Mandel, L. J. Potassium Transport in the Rabbit Renal Proximal Tubule: Effects of Barium, Ouabain, Valinomycin, and Other Ionophores. *J. Membr. Biol.* **1986**, *94*, 153−161.
(34) Vijayvergiya, C.; De Angelis, D.; Walther, M.; Kühn, H.; Duvoisin, R. M.; Smith, D. H.; Wiedmann, M. High-Level Expression of Rabbit 15-Lipoxygenase Induces Collapse of the Mitochondrial pH Gradient in Cell Culture. *Biochemistry* **2004**, *43*, 15296−15302.
(35) Catrina, I.; O'Brien, P. J.; Purcell, J.; Nikolic-Hughes, I.; Zalatan, J. G.; Hengge, A. C.; Herschlag, D. Probing the Origin of the Compromised Catalysis of *E. coli* Alkaline Phosphatase in its Promiscuous Sulfatase Reaction. *J. Am. Chem. Soc.* **2007**, *129*, 5760−5765.
(36) Jia, L.; Xu, J.-P.; Li, D.; Pang, S.-P.; Fang, Y.; Song, Z.-G.; Ji, J. Fluorescence Detection of Alkaline Phosphatase Activity with β-Cyclodextrin-modified Quantum Dots. *Chem. Commun.* **2010**, *46*, 7166−7168.